Interstitial Clusters

DOI: 10.1002/anie.201310436

A Novel Concept for the Synthesis of Multiply Doped Gold Clusters $[(M@Au_nM'_m)L_k]^{q+}$**

Arik Puls, Paul Jerabek, Wataru Kurashige, Moritz Förster, Mariusz Molon, Timo Bollermann, Manuela Winter, Christian Gemel, Yuichi Negishi, Gernot Frenking, and Roland A. Fischer**

Dedicated to Professor Hubert Schmidbaur on the occasion of his 80th birthday

Abstract: *Heterometal-doped gold clusters are poorly accessible through wet-chemical approaches and main-group-metal- or early-transition-metal-doped gold clusters are rare. Compounds $[M(AuPMe_3)_{11}(AuCl)]^{3+}$ (M = Pt, Pd, Ni) (**1**–**3**), $[Ni(AuPPh_3)_{(8-2n)}(AuCl)_3(AlCp^*)_n]$ (n = 1, 2) (**4**, **5**), and $[Mo(AuPMe_3)_8(GaCl_2)_3(GaCl)]^+$ (**6**) were selectively obtained by the transmetalation of $[M(M'Cp^*)_n]$ (M = Mo, E = Ga, n = 6; M = Pt, Pd, Ni, M' = Ga, Al, n = 4) with $[ClAuPR_3]$ (R = Me, Ph) and characterized by single-crystal X-ray diffraction and ESI mass spectrometry. DFT calculations were used to analyze the bonding situation. The transmetalation proved to be a powerful tool for the synthesis of heterometal-doped gold clusters with a design rule based on the 18 valence electron count for the central metal atom M and in agreement with the unified superatom concept based on the jellium model.*

Every atom counts in metal clusters. The composition of the core and ligand shell is crucial for the physical and chemical properties of clusters.[1] Gold is among the most thoroughly studied cluster metals and the famous "magic number" clusters $[Au_{13}(PMe_2Ph)_{10}Cl_2](PF_6)_3$ and $[Au_{55}(PPh_3)_{12}Cl_6]$,[2] discovered in 1981, are today's textbook examples. Au clusters are important for the study of metal–metal bonding and the understanding of the transition from the molecular size regime to the extended bulk phase, but they have also gained importance in catalysis, fuel cells, bio-sensing and labeling, and molecular electronics.[3] The incorporation of heteroatoms, that is, noble metals other than gold, is attractive because this doping leads to specific changes of the electronic structure and offers control of the properties.[4,5] However, cluster synthesis by wet chemistry is difficult, especially if heterometal atoms are included. A widely employed method to prepare doped Au clusters is the co-reduction of $[AuCl_4]^-$ with other metal salts in the presence of capping ligands. This concept works well for Pd and Pt as interstitial dopants and thiols as surface-capping groups, for example $[Pt@Au_{24}(SC_2H_4Ph)_{18}]$.[5] However, this strategy becomes increasingly problematic for less-noble metals and other choices of protecting ligands. The reactions exhibit poor selectivity and special separation techniques are required.[6] Alternative, chemoselective access to doped clusters $[M@Au_n]L_m$ is very rare.[7] In 2002, Li et al. described ligand-free $M@Au_{12}$ (M = Mo, W), experimentally proving Pyykkö's theoretical prediction of their unique stability.[8] A variety of $M@Au_n$ clusters were obtained by laser vaporization of a mixed Au/Mo (or Au/W) target into a stream of He carrier gas, monitored by time-of-flight mass spectrometry. The anions $[M@Au_{12}]^-$ were mass selected and characterized by photoelectron spectroscopy. Most of the current work on doped Au clusters is similar or purely theoretical and thus, possibly, quite far from applications. Our discovery of $[Mo(ZnCp^*)_3(ZnMe)_9]$ ($Cp^* = C_5Me_5$), in which the $Mo@Zn_{12}$ core displays striking similarities to the bonding situation of $M@Au_{12}$,[8,9] inspired us to design a novel wet-chemical access to $[M@Au_n]L_m$. The concept is based on our library of related molecules $[M@M'_a]R_a$ (a = 8–12; M = Mo, Ru, Rh, Ni, Pd, Pt; M' = Zn, Ga, Cd; R = Me, Et, Cp*)[10] and features the multiple transmetalation reaction depicted in Scheme 1. Note the isolobal relationship $ZnR \leftrightarrow AuPR'_3$ (both are one-electron

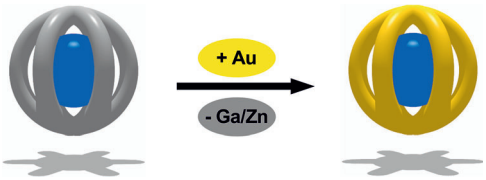

Scheme 1. Transmetalation concept for interstitial gold clusters of formula $[M@Au_n]L_m$. The interstitial M atom (blue) is transfered from the cage M'_a of the precursor compound $[M(M'R)_a]$ into the golden cage Au_n of the M-doped Au cluster (ligand surface capping not shown).

[*] A. Puls, M. Molon, Dr. T. Bollermann, M. Winter, Dr. C. Gemel, Prof. Dr. R. A. Fischer
Anorganische Chemie II - Organometallics & Materials
Fakultät für Chemie und Biochemie
Ruhr-Universität Bochum
44801 Bochum (Germany)
E-mail: roland.fischer@rub.de

P. Jerabek, M. Förster, Prof. Dr. G. Frenking
Fakultät für Chemie, Philipps-Universität Marburg
35032 Marburg (Germany)
E-mail: frenking@chemie.uni-marburg.de

W. Kurashige, Prof. Dr. Y. Negishi
Department of Applied Chemistry, Faculty of Science, Tokyo University of Science
Shinjuku-ku, Tokyo, 162-8601 (Japan)

[**] A.P. is grateful for a scholarship from the Fonds of the Chemical Industry (Germany) and for financial support from the Ruhr-University Research School and the German Academic Exchange Service (DAAD).

Supporting information for this article is available on the WWW under http://dx.doi.org/10.1002/anie.201310436.

ligands). The validity of the 18 valence electrons (18 ve) rule[9] for (blue) M embedded in the ligand shell of (gray) M′ or (yellow) Au suggests the substitution rule of one Zn atom by one Au or two Au atoms for one Al or Ga atom during transmetalation. Herein we present our results showing that this concept is working indeed.

The new compounds listed in Table 1 were synthesized by reaction of $[ClAuPR_3]$ ($PR_3 = PMe_3$, PPh_3) with $[M(GaCp^*)_4]$ (M = Ni, Pd, Pt) leading to **1–3**, with $[Ni(AlCp^*)_4]$ leading to **4** and **5**, and with $[Mo(GaCp^*)_6]$ leading to **6** in CH_2Cl_2 solution

Table 1: The new compounds **1–6**: numbering scheme, formulas, core composition, and idealized point group symmetry (S).

	Composition	Core	S
1	$[Pt(AuPMe_3)_{11}(AuCl)][GaCl_4]_3$	$Pt@Au_{12}$	C_{5v}
2	$[Pd(AuPMe_3)_{11}(AuCl)][GaCl_4]_3$	$Pd@Au_{12}$	C_{5v}
3	$[Ni(AuPMe_3)_{11}(AuCl)][GaCl_4]_3$	$Ni@Au_{12}$	C_{5v}
4	$[Ni(AuPPh_3)_6(AuCl)_3(AlCp^*)]$	$Ni@Au_9Al$	C_{3v}
5	$[Ni(AuPPh_3)_4(AuCl)_3(AlCp^*)_2]$	$Ni@Au_7Al_2$	C_1
6	$[Mo(AuPMe_3)_8(GaCl_2)_3(GaCl)][GaCl_4]$	$Mo@Au_8Ga_4$	C_1

(up to 30% yield of isolated product; for experimental details see the Supporting Information). The air-stable compounds **1–3** were purified by column chromatography while the high reactivity of **4–6** required manual separation of the crystals from the by-products under inert atmosphere. Notably, the neutral $[Mo(AuPPh_3)_8(AuCl)_2(GaMe)_2]$ (**7**, similar to the cluster cation of **6**), results from the reaction of $[Mo(GaMe)_4(ZnCp^*)_4]$ with $[ClAuPPh_3]$ (Figure S16). We did, however, not include cluster **7** in the discussion, due to the ambiguity in assigning Zn/Ga by single-crystal X-ray diffraction (similar scattering contrast) and difficulties in obtaining pure samples of satisfactory analysis (impurity: $[Au(PPh_3)_2][Zn_2Cl_6]$). Nevertheless, the $Mo@Au_{10}Ga_2$ core of **7** with interstitial Mo and additional shell-doping Ga may be regarded as the closest approximation to the neutral (ligand-free) $M@Au_{12}$ species (M = Mo, W) that we could isolate so far.[8]

Figure 1 highlights representative structures obtained by single-crystal X-ray diffraction (XRD). The cluster cation of **1**[11] (Figure 1a) reveals an almost perfect, icosahedral $Pt@Au_{12}$ unit (C_{5v}), which is surface-capped by eleven PMe_3 ligands and one Cl ligand (cluster cations of **2** and **3** are isostructural; Figures S4 and S7). The $d_{Au\text{-}P}$ and $d_{Au\text{-}Cl}$ bond lengths are within the expected range.[7c,d] The $d_{Pt\text{-}Au}$ separations are very similar (Pt(1)-Au(1) 2.741(1) Å for AuCl; 2.705(1)–2.763(1) Å for the $Au(PMe_3)$ groups) and agree with value of 2.75 Å reported for $[Pt@Au_{24}(SC_2H_4Ph)_{18}]$[5b] and with $d_{Pt\text{-}Au}$ separations in intermetallic phases (2.744–2.778 Å).[12] All known clusters $[Pt@Au_n]L_m$ have fewer Au atoms ($n \leq 10$) and shorter $d_{Pt\text{-}Au}$ separations (2.640(1)–2.725(1) Å).[7e–g] High-resolution mass spectra (HRMS) of **1–3** were obtained by using a FT-ICR instrument and the electrospray ionization technique (ESI; Figures S2, S5, and S8).[13] Molecular ion (MI) peaks MI^{3+} were found at $m/z =$ 1143.66 for **1**, 1114.11 for **2**, and 1098.20 for **3** and the isotopic patterns are in perfect agreement with the compositions derived from XRD (Table 1). The adducts $[MI]^{3+}[GaCl_4]^-_n$ ($n = 1, 2$) were detected in the case of **1.** Other fragments were

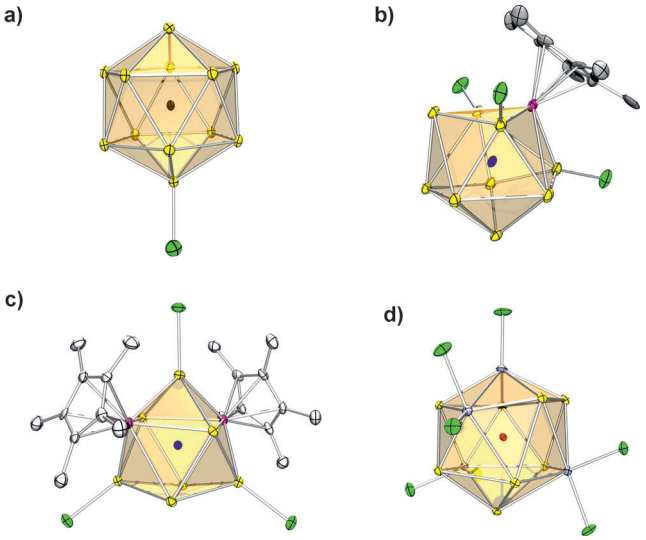

Figure 1. Molecular structures of representative cluster cores in the solid state (Table 1): a) $Pt@Au_{12}$ (**1**), b) $Ni@Au_9Al$ (**4**), c) $Ni@Au_7Al_2$ (**5**), and d) $Mo@Au_8Ga_4$ (**6**) (Povray plot; thermal ellipsoids are shown at the 50% probability level, hydrogen atoms and phosphine ligands are omitted for clarity. Au yellow, Mo red, Ni blue, Ga light blue, Al purple, Pt brown, Cl green, C white. For further details see the Supporting Information).

monitored as well, and the by-product $[Au(PMe_3)_2]^+$ was the only assignable species. In the negative mode the anion $[GaCl_4]^-$ was the only observable species for **1–3**. The ^{31}P NMR spectra of **1–3** in solution (Figure S19a) reveal one signal (fluctional PMe_3 or exchange) while the solid-state ^{31}P MAS-NMR spectra show three distinct signals in keeping with the C_{5v} symmetry. The $\delta(^{31}P)$ [ppm] shifts exhibit a clear trend: 25.71 (Pt), 20.74 (Pd), 13.90 (Ni). In the UV/Vis spectra (Figure S19b) a strong dependence of the absorption on the nature of M is observed: M = Pt: 407 nm; Pd: 447 nm; Ni: 471 nm. This is due to gradual modulation of the electronic structure in the series. The IR spectra indicate only little influence of the core doping on the vibrational modes (Figure S19d).

The new synthesis concept of multiple transmetalation not only gives access to "homoleptic" $M@Au_{12}$ with one interstitial heterometal atom M but also allows doping of the cluster Au shell around M with another M′. Thus, $Ni@Au_9Al$ (**4**) and $Ni@Au_7Al_2$ (**5**) are shell-doped with Al atoms, while $Mo@Au_8Ga_4$ (**6**) is shell-doped with Ga. The heterometallic cluster shell and the heteroleptic ligand sphere, with bulky Cp* ligands exclusively binding to the Al and Ga centers, lead to distortions of the clusters **4–6** from ideal polyhedra. However, each structure can be quantitatively related to an ideal body by means of the Continuous Shape Measures method (CShM, $S_Q(P)$).[14] Thus, $Ni@Au_7Al_2$ (**5**) comes close to a regular tricapped trigonal prism ($S_Q(P) = 0.47$), while $Mo@Au_8Ga_4$ (**6**) is best described as a distorted icosahedron ($S_Q(P) = 0.84$). The distortions are larger for $Ni@Au_9Al$ (**4**), which is a usual feature for polyhedra with ten vertices (centaur polyhedron ($S_Q(P) = 1.48$) or bicapped square antiprism ($S_Q(P) = 1.52$)). All clusters adapt the arrangement of the capping ligands with the highest symmetry.

In **4**,[11] the Ni atom is surrounded by one AlCp*, three AuCl, and six $AuPPh_3$ groups in overall C_{3v} symmetry (Figure 1b). The Au–Cl units are vicinal to the bulky AlCp* moiety, leading to significant bending of Ni-Au-Cl angles (164.18(2)°–170.18(2)°). Also, the Ni-Au-P angles deviate from linearity (163.82(2)°–175.72(2)°). The $d_{Au\text{-}Cl}$ and $d_{Au\text{-}P}$ distances are comparable to those in other interstitial (M) and PR_3-protected Au clusters.[7] The Ni(1)-Al(1) distance of 2.352(6) Å is significantly longer than that in $[Ni(AlCp^*)_4]$ (2.173(1) Å).[15] The $d_{Au\text{-}Al}$ distances range between 2.596(6) and 2.633(6) Å and the $d_{Ni\text{-}Au}$ distances are between 2.537(2) and 2.700(2) Å. Ni and Au are immiscible in the bulk phase. Ternary phases Ni/Au/Al are known; however, they exhibit an Al_2Au-type lattice with Ni partially substituting for Au and the observed typical $d_{Ni\text{-}Au}$ distances of 2.57 Å match bond lengths in **4** and **5** very well.[16]

The tricapped trigonal-prismatic cluster of **5**[11] (Figure 1c) is constructed of two $AlAu_2$ triangles, which are face-capped by three AuCl vertices. The cluster lacks a symmetry element and the structure is chiral. The enantiomeric mixture of **5** crystallizes in the achiral space group $P2_1/c$ with one molecule per asymmetric unit (Figures S11–S13). The Ni atom is surrounded by four $AuPPh_3$, three AuCl, and two AlCp* ligands. Again, the $d_{Au\text{-}P}$ and $d_{Au\text{-}Cl}$ separations have typical values.[7] The Ni-Al-Cp* units are almost linear (Ni(1)-Al(1)-$Cp^*_{Centroid}$(1) 178.74°, Ni(1)-Al(2)-$Cp^*_{Centroid}$(2) 178.99°) while the Ni-Au-Cl units deviate slightly (172.70(5)°–177.35(5)°) and the Ni-Au-P units (166.99(5)°–176.75(5)°) even more from linearity. The distances Ni(1)-Al(1/2) (2.283(2) Å and 2.265(2) Å) are shorter than those in **4**. Interestingly, two distinct sets of $d_{Al\text{-}Au}$ distances are found: the contacts Al–AuCl (2.650(2)–2.694(2) Å) are shorter than the contacts Al–Au(PPh_3) (2.957(2)–3.152(2) Å). The $d_{Ni\text{-}Au}$ separations are in the range 2.492(1)–2.537(1) Å and similar to those in **4**.

The cluster cation of **6**[11] represents a distorted icosahedron, whose Mo center is surrounded by eight Au(PMe_3), three $GaCl_2$, and one GaCl moiety in overall C_1 symmetry. The $d_{Mo\text{-}Au}$ separations are between 2.735(1)–2.811(1) Å and hence agree well with the value calculated for the I_h-symmetric gas-phase species $Mo@Au_{12}$ (2.757 Å).[8] Notably, no Au/Mo alloy phases are known due to immiscibility of the bulk metals.[17] The tangential distances $d_{Au\text{-}Au}$ ($\varnothing$ = 2.939 Å) of **6** are also very similar to those in $Mo@Au_{12}$ (2.898 Å). The $d_{Au\text{-}Ga}$ distances of 2.575(2)–3.084(2) Å compare with those in $[Au_3(\mu\text{-}GaI_2)_3(GaCp^*)_5]$ (2.377(2)–2.620(1) Å) and are also similar to the that in the intermetallic phase $AuGa_2$ (2.63 Å).[18] The $d_{Mo\text{-}Ga}$ separations are longer for the $GaCl_2$ vertices (Mo(1)-Ga(2) 2.671(2), Mo(1)-Ga(3) 2.647(2), Mo(1)-Ga(4) 2.666(2) Å) than for the GaCl vertex (Mo(1)-Ga(1) 2.504(2) Å). All four Mo–Ga bonds are elongated with respect to the homoleptic $[Mo(GaCp^*)_6]$ (2.384(1)–2.493(1) Å).[19] The Mo-Au-P angles deviate only slightly from linearity ($\varnothing$ = 173.90°) with typical $d_{Au\text{-}P}$ values ($\varnothing$ = 2.310 Å).[7h,i]

Most likely steric crowding of the capping groups (PR_3, Cp*) and the presence of much less bulky and noninnocent, nucleophilic counterions such as Cl^-, which is introduced by the choice of the gold component $[ClAuPR_3]$, are the reasons for the inaccessibility of the clusters $\{[M@Au_{12}](PR_3)_{12}\}^{q+}$ (M = Mo, q = 0; M = Ni, Pt, Pt; q = 4) exhibiting a homoleptic ligand shell. The electronic situation (see below) may require a charge q of the clusters. Thus, the cage metal atoms Au, Al, or Ga are to some extent electrophilic, which favors Lewis acid/base interactions. Therefore it is clear that in case of the Au/Ga mixed shell of **6**, the more electrophilic (hard) sites are the Ga centers, which bind Cl^- and the soft PR_3 ligands bind to Au centers. The fact that the binding of the Cp* ligand to Al in AlCp* is stronger (more ionic) than the analogous binding in GaCp* together with the effects of steric crowding are reflected by the preferred incorporation of Cp* in **4** and **5** at the Al site, while in the Au/Ga mixed cluster **6** the Cl coordination to Ga is preferred over surface-capping with Cp*.

Pyykkö pointed out that the 18 electron rule applied in coordination chemistry is also valid for gold clusters Au_n and $M@Au_n$, that is, $W@Au_{12}$ (Au is a one-electron ligand/donates one electron to the cluster).[20] In order to quantitatively analyze the bonding situations in the new M- and M′-doped Au-clusters **1**–**6** and aiming at a comparison with the related 18 ve compounds $[M(M'R)_a]$,[9,10] we carried out DFT calculations at the BP86/TZVPP level on the model compounds **1M**–**6M** (PMe_3 and PPh_3 are replaced by PH_3). Their optimized structures are in good agreement with the data for the real systems (Tables S13–S16). The electronic structures were analyzed by Energy Decomposition Analysis with Natural Orbitals of Chemical Valency (EDA-NOCV).[21] Theses calculations provide detailed information about the bonding situation in the molecules (Table 2, Figure 2). The interaction energies ΔE_{int} between the central M and the cage $\{Au_{12}(PH_3)_{11}Cl\}^{3+}$ (Au_{12}) of **1M**–**6M** exhibit the familiar V-shaped trend Pd < Ni < Pt.[22] The bonding comes mainly from electrostatic attractions ΔE_{elstat} while the orbital (covalent) interactions ΔE_{orb} provide 28–35% of the total attraction. Inspection of the deformation densities $\Delta\rho$ of the pairwise metal–cage interactions makes it possible to assign each term to a particular orbital interaction with the associated charge flow and stabilization energy. Figure 2 displays as representative examples the charge flow of **1M** from the occupied cage orbitals to the vacant valence s atomic orbital of Pt (left) and from one occupied valence d atomic orbital of Pt to a vacant cage orbital (right). Table 2 shows that the largest overall contribution to the orbital term comes from the donation of the valence d electrons of M to the vacant d-like orbitals of the Au_{12} cage. Note that the backdonation $Au_{12}\rightarrow$s from the occupied cluster orbital into the vacant s atomic orbitals of the central metal atom in **1M** and **3M** is as strong as a single d$\rightarrow$$Au_{12}$ donation ,which shows that the strength of the donation and backdonation is not primarily related to the charge of the fragments but to the orbital occupation. The individual $Au_{12}\rightarrow$p backdonation is much weaker than the orbital interactions that involve the s and d valence atomic orbitals. This result has been found before.[9,20,23] The overall bonding situation of the interstitial Ni clusters **4M** and **5M** turned out to be very similar to that found in **3M** with the donation cage$\rightarrow$s(Ni) being only slightly weaker. This kind of computational analysis (EDA-NOCV) agrees with the empirical design rule of the compounds based on the 18 ve count of

Table 2: EDA-NOCV results for **1M**–**3M** (BP86/TZ2P+). Energies in kcal mol^{-1}. The interacting fragments are the cage $\{Au_{12}(PH_3)_{11}Cl\}^{3+}$ in the singlet state and the central M atom with the electron configuration $s^0p^0d^{10}$.

	1M	2M	3M	
ΔE_{Int}	−245.4	−178.0	−224.4	
ΔE_{Pauli}	457.0	379.4	279.6	
ΔE_{elstat}	−493.1 (70.2%)	−403.8 (72.2%)	−328.4 (65.2%)	
ΔE_{orb}	−209.2 (29.8%)	−155.6 (27.8%)	−175.6 (34.8%)	
$\Delta E_{orb\ (a)}$	−30.5 (14.6%)	−25.1 (16.1%)	−30.7 (17.5%)	$d\rightarrow Au_{12}$
$\Delta E_{orb\ (b)}$	−30.4 (14.5%)	−25.0 (16.1%)	−30.7 (17.5%)	$d\rightarrow Au_{12}$
$\Delta E_{orb\ (c)}$	−29.7 (14.2%)	−24.6 (15.8%)	−30.5 (17.4%)	$d\rightarrow Au_{12}$
$\Delta E_{orb\ (d)}$	−27.6 (13.2%)	−22.2 (14.3%)	−25.2 (14.4%)	$d\rightarrow Au_{12}$
$\Delta E_{orb\ (e)}$	−27.6 (13.2%)	−22.2 (14.2%)	−25.2 (14.4%)	$d\rightarrow Au_{12}$
$\Delta E_{orb\ (f)}$	−29.4 (14.1%)	−11.8 (7.6%)	−25.3 (14.4%)	$Au_{12}\rightarrow s$
$\Delta E_{orb\ (g)}$	−7.3 (3.5%)	−5.1 (3.3%)	−5.7 (3.2%)	$Au_{12}\rightarrow p$
$\Delta E_{orb\ (h)}$	−7.2 (3.4%)	−5.0 (3.2%)	−5.6 (3.2%)	$Au_{12}\rightarrow p$
$\Delta E_{orb\ (i)}$	−7.2 (3.4%)	−5.0 (3.2%)	−5.6 (3.2%)	$Au_{12}\rightarrow p$
$\Delta E_{orb(res)}$	−12.3 (5.9%)	−9.6 (6.2%)	−8.9 (5.1%)	

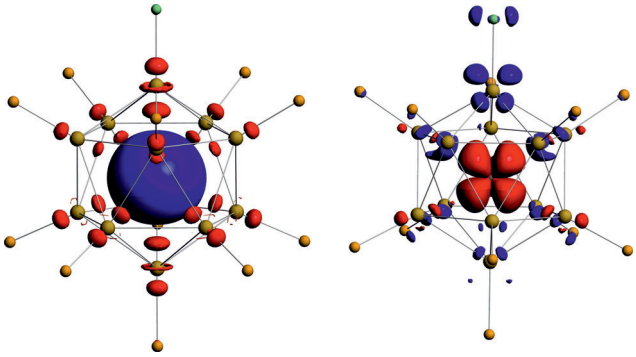

Figure 2. Examples for the deformation densities $\Delta\rho$ of **1M** (BP86/TZ2P+), red: electron depletion; blue: electron accumulation; left: $\Delta E_{orb(f)} = -29.4$ eV for $Au_{12}\rightarrow$s; right: $\Delta E_{orb(f)} = -27.6$ eV for d$\rightarrow$ Au_{12}.[24]

the interstitial metal atom M in $\{[M@Au_nM'_m]L_k\}^{q+}$ ($k \geq n+m \geq 9$). This means that **1**–**6** should be treated more like coordination compounds similar to $[M(M'R)_a]$ rather than rigorously as clusters.[10,20]

Alternatively, **1**–**6** can be regarded as derivatives of clusters like $[Au_{13}(PPhMe_2)_{10}Cl_2]^{3+}$ and thus should fulfill the cluster valence electron (cve) counting rule of the unifying superatom concept based on the jellium model for $\{[Au_nX_p]L_k\}^{q+}$ (X = halide, thiolate; L = phosphine, etc.): $cve = nv_A - p - q$; with $v_A = 1$ for Au (effective electronic valence).[25,26] Accordingly, a spherical Au_{13} cluster requires cve = 8 for $1S^2$ and $1P^6$ jellium shell closing and compounds $[M@Au_{11}(PMe_3)_{11}(AuCl)]^{3+}$ (**1**–**3**) follow this rule with v_A-(d^{10}M) = 0. The same is derived for **4**–**6** with v_A(Al/Ga) = 3 and accounting for d^6Mo (withdrawal of four electrons for Mo d-shell closing; Table S11). Interestingly, **1**–**6** feature some perturbation of the idealized Au_{13} bonding situation as indicated by the slight widening of $d_{Au\text{-}Au}$ separations within the cages (Table S12). Full details of the bonding analysis and comparisons with $[M(M'R)_a]$ and the relation to other gold clusters described by the jellium model will be given elsewhere.[24]

In summary, we have demonstrated a novel concept (Scheme 1) for the synthesis of multiply metal-doped ligand-stabilized small Au clusters, also with the introduction of unusual doping metals such as Mo, Ni, Al, and Ga. It follows from our data and discussion that the capping ligands X and L, introduced through the component [XAuL], may allow control of the transmetalation reaction to also yield other clusters beyond those listed in Table 1. For example: replacing Cl by more weakly coordinating anions X (e.g. $CF_3SO_3^-$) and modifying PR_3 or choosing different neutral capping ligands L such as isonitriles CNR or nitrogen heterocyclic carbenes for the Au component [XAuL]. On the other side, a growing library of M- and M′-transfer reagents are at hand, including compounds such as $[M(M'R)_n]$ and $[M(M''R)_a(M'R)_b]$, oligonuclear $[M_a(M'Cp^*)_b]$, and heteroleptic $[(R_3P)_aM(M'Cp^*)_b]$.[10] This broad spectrum of available reagents opens plenty of opportunities to further explore our synthesis concept for multiply metal-doped Au clusters.

Experimental Section

1–**3**: Samples of freshly prepared $[M(GaCp^*)_4]$ (M = Pt, Pd, Ni) (0.065 mmol) and $[ClAuPMe_3]$ (0.240 g, 0.777 mmol) were suspended in 10 mL of CH_2Cl_2. The reaction mixture was stirred for 24 h at room temperature, whereupon a yellowish metallic residue precipitated. The reaction solution was filtered off and concentrated. Samples were purified by column chromatography on Al_2O_3 (eluent: CH_2Cl_2/CH_3OH 12.5:1). Hexane was used to precipitate an orange-red solid. After drying in vacuo pure orange-red crystals were obtained by recrystallization from CH_2Cl_2 (diffusion of overlaying *n*-hexane). Yields: 20–30%. For the related synthesis of **4**–**7** and additional characterization data see the Supporting Information.

Received: December 2, 2013
Published online: April 2, 2014

Keywords: Au · cluster compounds · interstitial clusters · one-electron donor · transition-metal doping

[1] a) M. Akutsu, K. Koyasu, J. Atobe, N. Hosoya, K. Miyajima, M. Mitsui, A. Nakajima, *J. Phys. Chem. A* **2006**, *110*, 12073–12076; b) H. Qian, M. Zhu, Z. Wu, R. Jin, *Acc. Chem. Res.* **2012**, *45*, 1470–1479.

[2] a) C. E. Briant, B. R. C. Theobald, J. W. White, L. K. Bell, D. M. P. Mingos, *J. Chem. Soc. Chem. Commun.* **1981**, 201–202; b) G. Schmid, R. Pfeil, R. Boese, F. Bandermann, S. Meyer, G. H. M. Calis, J. W. A. van der Velden, *Chem. Ber.* **1981**, *114*, 3634–3642.

[3] a) Y. Zhu, H. Qian, R. Jin, *J. Mater. Chem.* **2011**, *21*, 6793–6799; b) W. Tang, S. Jayaraman, T. F. Jaramillo, G. D. Stucky, E. W. McFarland, *J. Phys. Chem. C* **2009**, *113*, 5014–5024; c) R. Wilson, *Chem. Soc. Rev.* **2008**, *37*, 2028–2045; d) N. Lu, J. Zheng, M. Gleiche, H. Fuchs, L. Chi, *Nano Lett.* **2002**, *2*, 1097–1099.

[4] a) N. K. Chaki, H. Tsunoyama, Y. Negishi, H. Sakurai, T. Tsukuda, *J. Phys. Chem. C* **2007**, *111*, 4885–4888; c) Y. Negishi, W. Kurashige, Y. Niihori, K. Nobusada, *Phys. Chem. Chem. Phys.* **2013**, *15*, 18736–18751; d) C. Kumara, A. Dass, *Nanoscale* **2012**, *4*, 4084–4086.

[5] a) H. Qian, D. Jiang, G. Li, C. Gayathri, A. Das, R. Gil, R. Jin, *J. Am. Chem. Soc.* **2012**, *134*, 16159 – 16162; b) S. L. Christensen, M. A. MacDonald, A. Chatt, P. Zhang, *J. Phys. Chem. C* **2012**, *116*, 26932 – 26937.

[6] a) R. Sardar, A. M. Funston, P. Mulvaney, R. W. Murray, *Langmuir* **2009**, *25*, 13840 – 13851; b) T. G. Schaaff, G. Knight, M. N. Shafigullin, R. F. Borkman, R. L. Whetten, *J. Phys. Chem. B* **1998**, *102*, 10643 – 10646; c) V. L. Jimenez, M. C. Leopold, C. Mazzitelli, J. W. Jorgenson, R. W. Murray, *Anal. Chem.* **2003**, *75*, 199 – 206; d) Y. Negishi, Y. Takasugi, S. Sato, H. Yao, K. Kimura, T. Tsukuda, *J. Am. Chem. Soc.* **2004**, *126*, 6518 – 6519.

[7] a) M. Laupp, J. Strähle, *Angew. Chem.* **1994**, *106*, 210 – 211; *Angew. Chem. Int. Ed. Engl.* **1994**, *33*, 207 – 209. b) – i) additional pertinent references: see Supporting Information.

[8] a) P. Pyykkö, N. Runeberg, *Angew. Chem.* **2002**, *114*, 2278 – 2280; *Angew. Chem. Int. Ed.* **2002**, *41*, 2174 – 2176; b) X. Li, B. Kiran, J. Li, H.-J. Zhai, L.-S. Wang, *Angew. Chem.* **2002**, *114*, 4980 – 4983; *Angew. Chem. Int. Ed.* **2002**, *41*, 4786 – 4789.

[9] T. Cadenbach, T. Bollermann, C. Gemel, I. Fernandez, M. von Hopffgarten, G. Frenking, R. A. Fischer, *Angew. Chem.* **2008**, *120*, 9290 – 9295; *Angew. Chem. Int. Ed.* **2008**, *47*, 9150 – 9154.

[10] a) T. Bollermann, C. Gemel, R. A. Fischer, *Coord. Chem. Rev.* **2012**, *256*, 537 – 555; b) M. Molon, C. Gemel, M. von Hopffgarten, G. Frenking, R. A. Fischer, *Inorg. Chem.* **2011**, *50*, 12296 – 1230.

[11] Crystal data for **1**, **4**, and **5** were obtained at 113(2) K with an Oxford Excalibur 2 diffractometer and $Mo_{K\alpha}$ radiation (λ = 0.71073 Å). **1**: $PtAu_{12}P_{11}Ga_3C_{34}H_{101}Cl_{15}$; M_r = 4150.42; orthorhombic; space group *Pna*2(1); Z = 4; a = 19.7506(7), b = 25.7976(6), c = 17.8562(5) Å, $\alpha=\beta=\gamma$ = 90°, V = 9098.1(5) Å^3; $\rho_{calc.}$ = 3.030 mg mm^{-3}; μ = 22.323 mm^{-1}; T = 113(2) K; $2\theta_{max}$ = 55.12°; 150635 reflections measured, of which 20826 were independent, R_{int} = 0.1570; The final values for $R1$ and $wR2$ were 0.0404 and 0.0723 [$I > 2\sigma(I)$]; Largest diff. peak/hole 2.71/−2.66 e Å^{-3}. **4**: $NiAu_9P_6AlC_{119}H_{107}Cl_5$; M_r = 3758.50; triclinic; space group $P\bar{1}$; Z = 2; a = 14.6468(4), b = 16.5588(5), c = 24.9024(7) Å, α = 88.187(2)°, β = 87.101(2)°, γ = 80.385(3)°, V = 5945.5(3) Å^3; $\rho_{calc.}$ = 2.099 mg mm^{-3}; μ = 11.457 mm^{-1}; T = 110(2) K; $2\theta_{max}$ = 58.08°; 66590 reflections measured, of which 27495 were independent, R_{int} = 0.1100; The final values for $R1$ and $wR2$ were 0.0738 and 0.1612 [$I > 2\sigma(I)$]; Largest diff. peak/hole 6.25/−3.84 e Å^{-3}. **5**: $NiAu_7P_4Al_2C_{96}H_{98}Cl_{11}$; M_r = 3257.01; monoclinic; space group $P2_1/c$; Z = 4; a = 16.5733(2), b = 19.9867(3), c = 30.0311(5) Å, $\alpha=\gamma$ = 90°, β = 90.5810(10)°, V = 9947.2(3) Å^3; $\rho_{calc.}$ = 2.175 mg mm^{-3}; μ = 10.889 mm^{-1}; T = 113(2) K; $2\theta_{max}$ = 55.12°; 199315 reflections measured, of which 22737 were independent, R_{int} = 0.0868; The final values for $R1$ and $wR2$ were 0.0348 and 0.0596 [$I > 2\sigma(I)$]; Largest diff. peak/hole 2.00/−1.65 e Å^{-3}. Data for **6** were obtained with an Oxford Supernova diffractometer and $Cu_{K\alpha}$ radiation (λ = 1.54184 Å): $MoAu_8Ga_5P_8C_{24}H_{72}Cl_{11}$; M_r = 3018.80; monoclinic; space group $P21/n$; Z = 4; a = 13.45026(18), b = 25.3314(3), c = 20.02384(18) Å, $\alpha=\gamma$ = 90°, β = 90.1494(11)°, V = 6822.39(13) Å^3; $\rho_{calc.}$ = 2.939 mg mm^{-3}; μ = 40.903 mm^{-1}; T = 101(2) K; $2\theta_{max}$ = 148.3°; 27661 reflections measured of which 11491 were independent, R_{int} = 0.0468; The final values for $R1$ and $wR2$ were 0.0415 and 0.1051 [$I > 2\sigma(I)$]; Largest diff. peak/hole 2.64/−2.73 e Å^{-3}; For all structures **1**, **4** – **6** full matrix least squares on F^2 was used as a refinement method. CCDC 970571 (**4**), 970572 (**6**), 970573 (**1**), and CCDC 970574 (**5**) contain the supplementary crystallographic data for this paper. These data can be obtained free of charge from The Cambridge Crystallographic Data Centre via www.ccdc.cam.ac.uk/data_request/cif.

[12] H. Okamoto, T. B. Massalski, *Bull. Alloy Phase Diagrams* **1985**, *6*, 46 – 57.

[13] D. Miura, J. Tsuji, K. Takahashi, H. Wariishi, K. Saito, *Anal. Chem.* **2010**, *82*, 5887 – 5891.

[14] a) H. Zabrodsky, S. Peleg, D. Avnir, *J. Am. Chem. Soc.* **1992**, *114*, 7843 – 7851; b) H. Zabrodsky, S. Peleg, D. Avnir, *J. Am. Chem. Soc.* **1993**, *115*, 8278 – 8289; c) M. Pinsky, D. Avnir, *Inorg. Chem.* **1998**, *37*, 5575 – 5582.

[15] B. Buchin, T. Steinke, C. Gemel, T. Cadenbach, R. A. Fischer, *Z. Anorg. Allg. Chem.* **2005**, *631*, 2756 – 2762.

[16] Z. Zhang, C. Zhang, Y. Gao, J. Frenzel, J. Sun, G. Eggeler, *Cryst. Eng. Comm.* **2012**, *14*, 8292 – 8300.

[17] M. M. Biener, J. Biener, R. Schalek, C. M. Friend, *Surf. Sci.* **2005**, *594*, 221 – 230.

[18] a) F. Weibke, E. Hesse, *Z. Anorg. Allg. Chem.* **1939**, *240*, 289 – 299; b) U. Anandhi, P. R. Sharp, *Angew. Chem.* **2004**, *116*, 6254 – 6257; *Angew. Chem. Int. Ed.* **2004**, *43*, 6128 – 6131.

[19] T. Bollermann, T. Cadenbach, C. Gemel, K. Freitag, M. Molon, V. Gwildies, R. A. Fischer, *Inorg. Chem.* **2011**, *50*, 5808 – 5814.

[20] a) P. Pyykkö, *J. Organomet. Chem.* **2006**, *691*, 4336 – 4340; b) P. Pyykkö, *Nat. Nanotechnol.* **2007**, *2*, 273 – 274.

[21] M. P. Mitoraj, A. Michalak, T. Ziegler, *J. Chem. Theory Comput.* **2009**, *5*, 962 – 970.

[22] a) G. Frenking, N. Fröhlich, *Chem. Rev.* **2000**, *100*, 717 – 765; b) M. Lein, G. Frenking, *Theory and Applications of Computational Chemistry*: *The First 40 Years* (Eds.: C. E. Dykstra, G. Frenking, K. S. Kim, G. E. Scuseria), Elsevier, Amsterdam, **2005**, pp. 367 – 411; c) G. Frenking, K. Wichmann, N. Fröhlich, C. Loschen, M. Lein, J. Frunzke, V. M. Rayón, *Coord. Chem. Rev.* **2003**, *238 – 239*, 55 – 91; d) M. Lein, A. Szabó, A. Kovács, G. Frenking, *Faraday Discuss.* **2003**, *124*, 365 – 381.

[23] A. Diefenbach, F. M. Bickelhaupt, G. Frenking, *J. Am. Chem. Soc.* **2000**, *122*, 6449 – 6461.

[24] A full account of the bonding analysis of **1M**–**6M** will be reported in a separate publication.

[25] H. Häkkinen, *Chem. Soc. Rev.* **2008**, *37*, 1847 – 1859.

[26] B. S. Gutrath, I. B. Oppel, O. Presly, I. Beljakov, V. Meded, W. Wenzel, U. Simon, *Angew. Chem.* **2013**, *125*, 3614 – 3617; *Angew. Chem. Int. Ed.* **2013**, *52*, 3529 – 3532.

